
EXPERIMENTAL PAPERS

The Electrophysiological Properties of Cortical Neurons in the Epileptic Foci of Children with Refractory Temporal Lobe Epilepsy

S. L. Malkin^{a,*}, V. A. Khachatryan^b, E. V. Fedorov^b, and A. V. Zaitsev^{a,b}

^a*Sechenov Institute of Evolutionary Physiology and Biochemistry, Russian Academy of Sciences, St. Petersburg, Russia*

^b*Almazov National Medical Research Centre, St. Petersburg, Russia*

*e-mail: adresatt@gmail.com

Received December 5, 2021

Revised December 20, 2021

Accepted December 21, 2021

Abstract—Temporal lobe epilepsy is a severe disorder of the central nervous system associated with an imbalance of excitation and inhibition in the brain, manifested by recurrent seizures. Approximately 30% of patients with epilepsy are pharmacoresistant, meaning that existing antiepileptic drugs can not completely control the seizures. One approach to treating refractory epilepsy is to surgically remove the seizure foci, usually located in the temporal cortex, hippocampus, or amygdala. This permits sustained remission in approximately 60–75% of cases. The study of morphological and functional features of neuronal networks in epileptic foci of patients with refractory temporal lobe epilepsy is necessary to understand the mechanisms of pathogenesis of this disease and to develop new approaches to its treatment. This study analyzed the electrophysiological properties of temporal cortex neurons obtained during surgical removal of epileptic foci in children with refractory temporal lobe epilepsy. The biophysical membrane properties of the neurons in brain slices were investigated using the patch-clamp method. We compared them with the properties of pyramidal neurons of the rat cortex. We found that human neurons are characterized by much higher excitability than rat neurons. They generate action potentials in response to minimal depolarization and maintain a high frequency of discharges. At the same time, they are characterized by a high membrane input resistance. The identified biophysical characteristics of neurons may underlie the pathological process leading to the generation of pharmacoresistant seizures in children with temporal lobe epilepsy.

DOI: 10.1134/S0022093022010197

Keywords: temporal lobe epilepsy, pyramidal neuron, human, action potential, cortex

INTRODUCTION

Epilepsy is the most prevalent disorder of the central nervous system, it affects around 1% of the

world population [1]. Despite the significant progress in the pharmacotherapy of epilepsy, up to 30% of its cases remain resistant to the currently available anticonvulsants [2]. The problem

Table 1. Patient data

No.	Sex	Age	Disease duration	Treatment	Removed area
1	M	11	4 years	Carbamazepine, Pantogam (N-pantoyl-GABA)	Anterior 2/3 of the right temporal lobe (4,3x3,7x3,1 cm), hippocampus
2	F	10	1 year	Carbamazepine, Convulex (Valproate)	Anterior areas of the left temporal lobe up to 4 cm from the pole
3	F	15	2 years	Trileptal (Oxcarbazepine), Keppra (Levetiracetam), Lamictal (Lamotrigine)	The left temporal lobe, posterior-lateral areas of the lower frontal gyrus, and upper-anterior areas of the upper parietal lobe
4	F	8	3 months	Depakine (Valproate), Keppra	Pole of the left temporal lobe up to 3,5 cm from the pole

of childhood refractory epilepsy is particularly urgent since uncontrolled seizures lead to different cognitive and psycho-emotional development impairments in children and a corresponding decrease in their quality of life [3]. The primary approach to treating refractory epilepsy in children is the surgical removal of the epileptic foci [4]. Although this approach leads to a stable remission in approximately 3/4 of the cases, some patients later experience seizure relapse due to the formation of a new epileptic focus [5]. Thus, investigating the pathogenetic mechanisms of refractory epilepsy remains an essential task.

The development of refractory epilepsy is linked to such morphological and network dysfunctions as hippocampal sclerosis, anomalous mossy fiber sprouting, blood–brain barrier disruption, and astrogliosis [6, 7]. Another disorder often associated with the refractory temporal lobe epilepsy in children is focal cortical dysplasia (FCD) [8]. There are known changes in the excitability of cortical pyramidal cells on the neuronal level in models of epilepsy in rats [9]. The hippocampal neurons of the adult temporal lobe epilepsy patients demonstrate the increased persistent Na^+ current amplitudes. However, the available data shows that the membrane properties of the neurons in the epileptic brain tissue are generally close to those of the healthy rat neurons [10]. Neurons in the temporal cortex of children with refractory epilepsy demonstrate similar characteristics [11]. However, the literary data on the neuronal mechanisms of refractory epilepsy in children is currently very sparse.

The age-related features of neocortical neurons in healthy humans and temporal lobe epilepsy patients are also underexplored. Thus, it has been shown that in rats, the neuronal input resistance is markedly reduced during the postnatal ontogenesis up to adolescence [12]. Such features may seriously impact the excessive excitation and anomalous synchronization mechanisms in the epileptic cortex; however, this question currently remains open. In this work, we studied the membrane properties of neurons in the temporal cortex of patients with childhood refractory temporal lobe epilepsy. The obtained data will help elucidate the features of this disorder in children.

MATERIALS AND METHODS

Patients

The study was conducted following the protocol approved by the Almazov National Medical Research Centre's ethical commission, developed based on the Helsinki declaration of 1964 and its subsequent updates. The parents of each patient included in the study gave their informed consent. Data obtained from 4 surgeries were included in the study (1 male and 3 female patients, Table 1). All patients were diagnosed with refractory temporal lobe epilepsy. After trying two or more pharmacological protocols, none of which were effective at seizure prevention, surgical removal of the epileptic foci from the temporal cortex was recommended. A structural anomaly of cortex and hippocampus linked to pharmacoresistant seizures was revealed for patient 4, so the surgical

treatment was suggested despite the relatively short duration of the illness. Clinical histological studies of the post-surgery material have shown the presence of type II or III focal cortical dysplasia (FCD) in all patients. The post-surgical examination included the MRI scans (Fig. 1), which allowed to document the precise localization of the removed brain region.

Preparation of the acute human brain slices

The brain tissue samples were obtained in the course of the neurosurgical removal of the epileptic foci in the temporal lobe of the patients of the pediatric neurosurgery division of the Almazov National Medical Research Centre. The localization of the pathological regions was clarified during the surgery using the electrocorticographic (ECoG) study. The pathological foci were characterized by the generation of the spike-wave activity patterns registered on the ECoG. To minimize the hypoxic damage to the removed cortical tissue, the surgeon kept their blood supply intact as long as possible and coagulated the vessels feeding them only immediately before their final removal. After the removal, the brain tissue was placed in the cooled to 0°C artificial cerebrospinal fluid (ACSF, in mM: 126 NaCl, 24 NaHCO₃, 2.5 KCl, 2 CaCl₂, 1.25 NaH₂PO₄, 1 MgSO₄, and 10 dextrose), and transported to the neurophysiological laboratory located in the IEPH RAS. The transportation time was 30–60 min. 300- μ m-thick slices were prepared using the Microm HM 650 V vibrating microtome (Microm International GmbH, Walldorf, Germany) in the cooled ACSF continually saturated with carbogen (5% CO₂ and 95% O₂). After the preparation, slices were placed in the room-temperature ACSF and incubated for 45 minutes. 5 to 10 slices from each patient were used for the experiments.

Preparation of the acute rat brain slices

Experiments were conducted on the 3-week-old male Wistar rats, which approximately corresponds to adolescence in humans [13].

The experimental procedures complied with the European Council Directive 86/609/EEC and approved by the bioethical commission the regulation for the use of the laboratory animals of IEPH RAS.

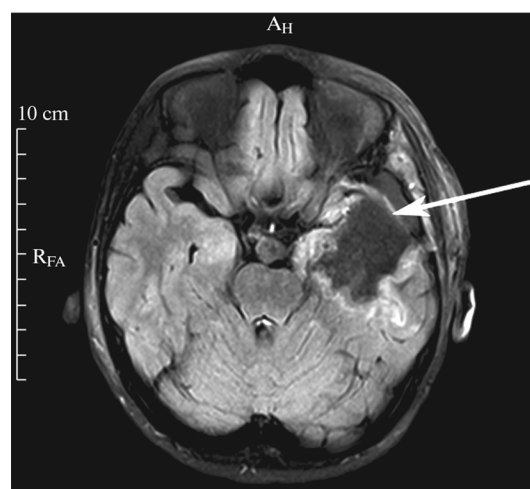


Fig. 1. Snapshot of the post-operational MRI for patient 2 following the surgery regarding the post-traumatic refractory epilepsy and type IIIB FCD. The arrow indicates the removed area in the anterior section of the left temporal lobe.

The rats were decapitated, their brains were quickly extracted and placed in the cooled Ringer solution aerated with the gas mixture of 95% O₂ + 5% CO₂. The 350- μ m-thick coronary brain slices were prepared similarly to the procedure described above for the human brain slices. The electrophysiological registration was performed in pyramidal neurons of the medial prefrontal cortex.

Electrophysiological registration

The electrophysiological registration of the neuronal properties was performed using the patch-clamp technique in the whole cell mode in a perfusion slice chamber kept at 30°C and perfused at a rate of 5 mL/min. The neurons in II–IV layers of the human temporal cortex were visualized using an Axioskop-2FS Plus microscope (Carl Zeiss AG, Oberkochen, Germany) equipped with differential interference contrast optics and a Sanyo VCB-3512P video camera (SANYO Electric Co., Ltd.; Moriguchi, Osaka, Japan). Glass electrodes with resistance 2–4 M Ω were filled with the following solution (in mM): 135 potassium gluconate, 5 KCl, 5 NaCl, 5 EGTA, 10 HEPES, 4 ATP-Mg, and 0.3 GTP-Na, pH 7.25. Passive and active membrane properties were studied by analyzing the neuronal responses to the current steps of 1.5 s length

applied every 3.5 s at the amplitudes ranged from -100 up to $+600$ pA at 10 pA step, which was enough to cause the depolarization block in all studied neurons.

The signals were registered using the EPC8 amplifier, digitized at 50 kHz using the analog-to-digital converter (ADC/DAC) LIH 8+8 and a PatchMaster 2x91 software (HEKA Elektronik GmbH, Ludwigshafen am Rhein, Germany). No online series resistance correction was applied.

Data analysis

The electrophysiological recordings were converted to the ABF format using the Review 5.0.2 software (Bruxton Corp., Seattle, WA, USA) and analyzed using a self-made program written in Python using NumPy [14], SciPy [15], pyqtgraph [16], and pyABF (<https://swharden.com/pyabf/>) libraries.

The action potentials (APs) generated in response to a rheobase current, i.e., minimal current sufficient to elicit the AP generation, were used to analyze the AP properties. We measured threshold, amplitude, afterdepolarization (ADP), fast and medium afterhyperpolarization (AHP), time to medium AHP peak, rise time, half-width, and width at the threshold level.

The threshold was determined as a point in which the first derivative from the potential by time (dV/dt) exceeded the threshold value of 5 mV/ms. The amplitude was determined as a peak value reached by the membrane potential during the AP generation relative to the threshold. ADP amplitude was defined as the membrane potential peak value at the section between the fast and medium AHP peaks relative to the fast AHP peak.

The fast AHP amplitude was determined as a point where the membrane potential decrease markedly slowed and became slower than 5 mV/ms. The medium AHP peak was measured at the point of the minimal membrane potential value, relative to the fast AHP peak. Time to medium afterhyperpolarization was measured between the fast and medium AHP peaks. Rise time was measured from 10% and 90% of the peak AP amplitude relative to the threshold. The AP duration (half-width) was measured at the level of its half-maximal amplitude.

The current-frequency curves were compared

using: (1) rheobase current—minimal current sufficient for the AP generation; (2) minimal current eliciting the maximal AP frequency; (3) minimal current eliciting the depolarization block of the AP generation; (4) time from the start of the depolarizing current to the first AP at the rheobase current; (5) maximal AP frequency; (6) maximal current-frequency curve slope; (7) early and late frequency adaptation values.

For each neuron, we plotted the current-frequency curves—the relation between the AP generation frequency and the amplitude of the injected current. Using these curves, we determined the maximal AP frequency and the rheobase current. To determine the maximal slope of the current-frequency curve, we approximated them with the Gompertz function:

$$y = a * e^{-b * e^{-c * x}},$$

where a is the upper asymptote (maximal frequency), b is the shift by the x-axis, c is the growth rate, and e is Euler's number.

The early frequency adaptation was calculated as the ratio between the second and the first interspike intervals, and the late adaptation—as the ratio between the last and the first intervals.

We measured a range of passive membrane properties of the neurons: resting membrane potential (RMP), input resistance (R_i), and membrane constant (τ). The resting membrane potential was measured as a mean value of the membrane potential on the trace with a zero injected current. The R_i was calculated as a slope of the linear section of the current-voltage relationship for the hyperpolarizing current steps. The potential was measured at the negative peak at the start of the step. The membrane constant was calculated as a parameter of the mono-exponential function with which we approximated the rising phase of the membrane potential in response to the 20 pA current step.

Statistical analysis

Statistical analysis was performed using the scripts written in Python programming language using Pandas (<https://pandas.pydata.org/>), NumPy, and SciPy libraries. Matplotlib [17] library was used for data visualization. One-way ANOVA was used for the comparisons between

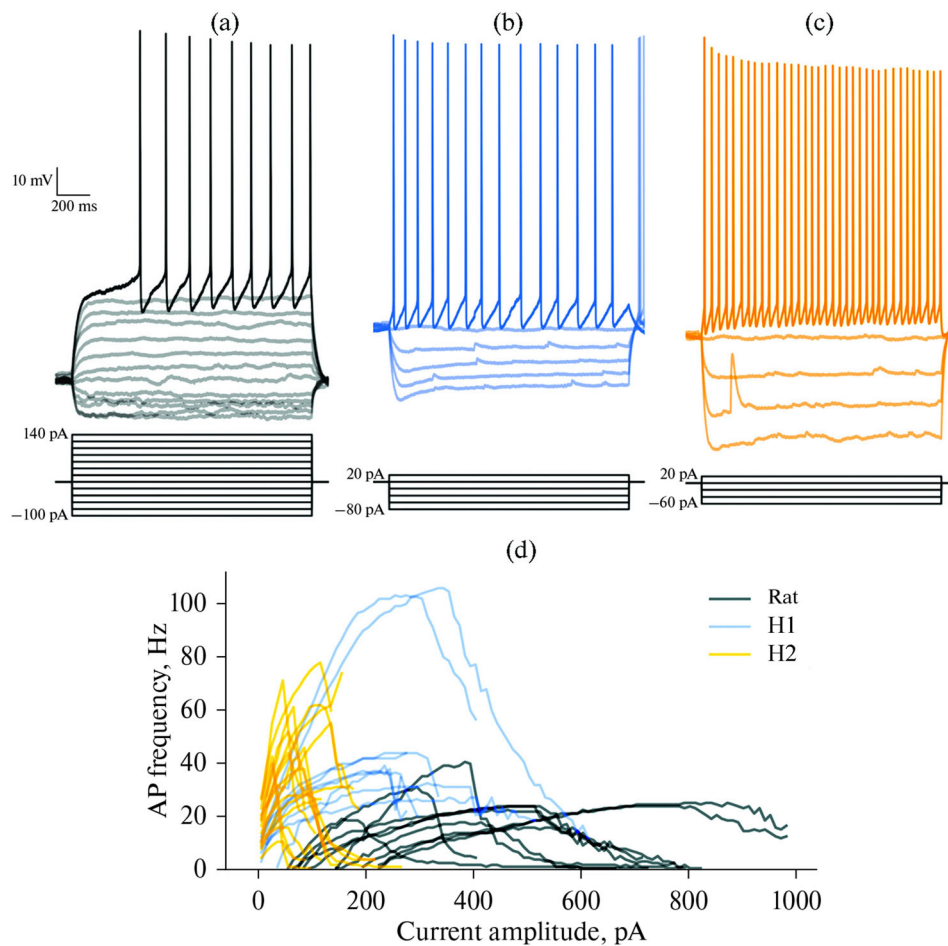


Fig. 2. Response patterns and current-frequency relationships of rat and human cortical neurons. Representative examples of responses of rat (a) and human (b, c) neurons. Rat—rat pyramidal neuron, H1—human type 1 neuron, H2—human type 2 neuron. (d) Current-frequency curves of the two human neuron subtypes (H1, $n = 9$; H2, $n = 17$), as well as rat pyramidal cells in medial prefrontal cortex ($n = 10$).

the three groups, with a Tukey's post hoc test for pairwise comparisons. The data are shown as mean \pm standard error.

RESULTS

The percentage of neurons suitable for the registration in human cortical slices was relatively small. Mainly small-sized neurons survived. When searching for the neurons to patch, preference was given to the neurons with a pyramidal shape and a visible apical dendrite. However, the presence of the apical dendrite was not always identifiable. Thus, the sample of the studied neurons may contain both excitatory pyramidal cells and inhibitory interneurons. All neurons included in the analysis had resting membrane potentials

below -50 mV, and their action potentials had an overshoot.

To compare the electrophysiological properties, we included in this work the recordings from rat cortical pyramidal neurons ($n = 10$) obtained in the same experimental setup in similar conditions.

Current-frequency curves of the neurons

Representative examples of the responses of human and rat neurons to the hyperpolarizing and depolarizing current are shown in Fig. 2. First, we plotted the current-frequency curves for each neuron—the relationships between the AP frequency and the amplitude of the depolarizing current. We observed the linear relationship between the current and the spike frequency at low current

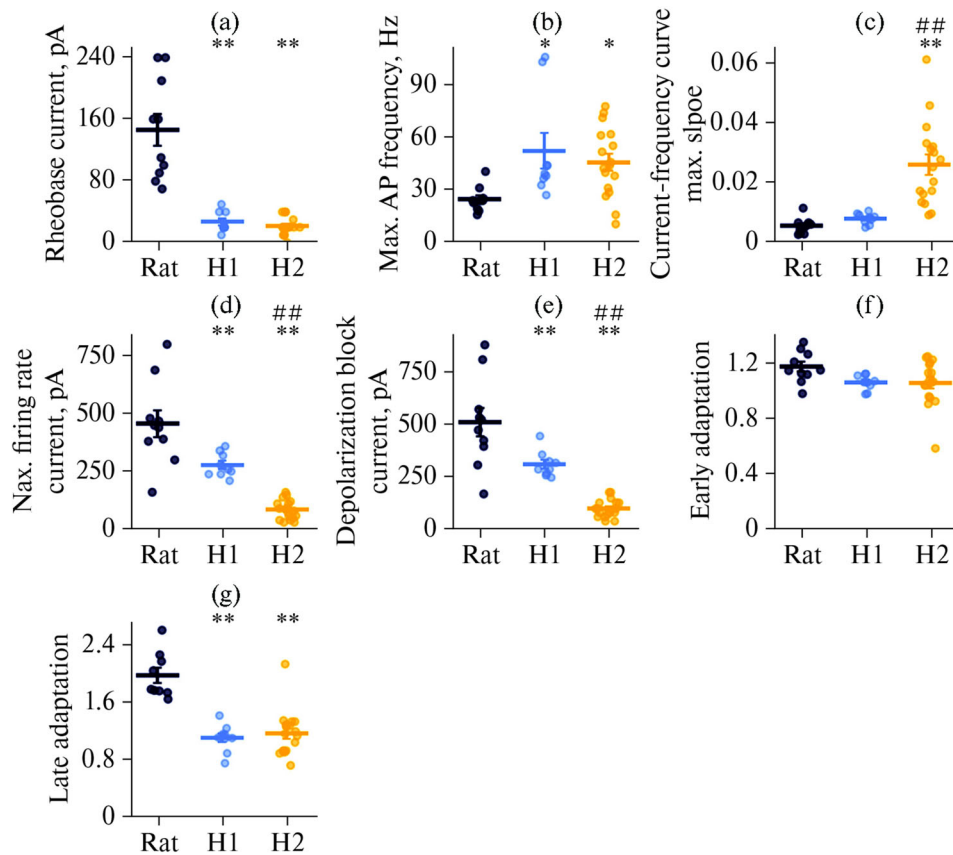


Fig. 3. Statistical data on the biophysical properties of human and rat neurons. (a) Rheobase current. $F_{2,33} = 42.7$, $p < 0.0001$; (b) Maximal AP frequency. $F_{2,33} = 5.03$, $p < 0.05$; (c) Maximal current-frequency curve slope. $F_{2,33} = 17.5$, $p < 0.0001$; (d) Minimal current eliciting the maximal AP frequency. $F_{2,33} = 42.6$, $p < 0.0001$; (e) Minimal current eliciting the depolarization block. $F_{2,33} = 37.8$, $p < 0.0001$; (f) Early AP frequency adaptation. $F_{2,33} = 2.7$, $p = 0.08$; (g) Late AP frequency adaptation. $F_{2,32} = 27.5$, $p < 0.0001$; *— $p < 0.05$, **— $p < 0.01$ —difference between rat and human neurons; ##— $p < 0.01$ —difference between H1 and H2 neurons (Tukey's post-hoc test).

amplitudes. In contrast, a further increase of the current amplitude leads to a stabilization of the AP frequency. Then a disruption of the AP generation occurs due to the depolarization block.

We observed that the current-frequency curves in human and rat neurons are significantly different (Fig. 2d). In rat neurons, the maximal AP frequency was lower; however, the AP generation was disrupted by higher currents than in human neurons.

The studied population of human neurons was heterogeneous by its current-frequency relationships. Thus, we divided the human neurons into two groups, one of which was characterized by a very low AP depolarization block threshold. The other one was able to generate the APs in a broader range of the injected currents. We chose the value of 200 pA as a nominal boundary. All

neurons that had not developed the depolarization block at the 200 pA current step were categorized as type 1 neurons (H1). The ones that had produced the depolarization block at the lower currents were classified as type 2 (H2).

Human type 2 neurons were characterized by a steep rise of AP frequency in response to the increase of the depolarizing current. Maximal current-frequency curve slope in this group of neurons was much higher than in H1 neurons and rat pyramidal cells (rat: 5.5 ± 0.8 Hz/ μ A ($n = 10$); H1: 8.0 ± 0.6 Hz/ μ A ($n = 9$); H2: 26.3 ± 3.4 Hz/ μ A ($n = 17$)). The H1 neurons were similar to the rat pyramidal cells by that metric (Figs. 2, 3c).

The rheobase current was approximately the same in both human neuron subtypes and several times lower than in rat pyramidal cells (rat: 146 ± 21 pA; H1: 27 ± 4 pA; H2: 21 ± 3 pA; Fig. 3a).

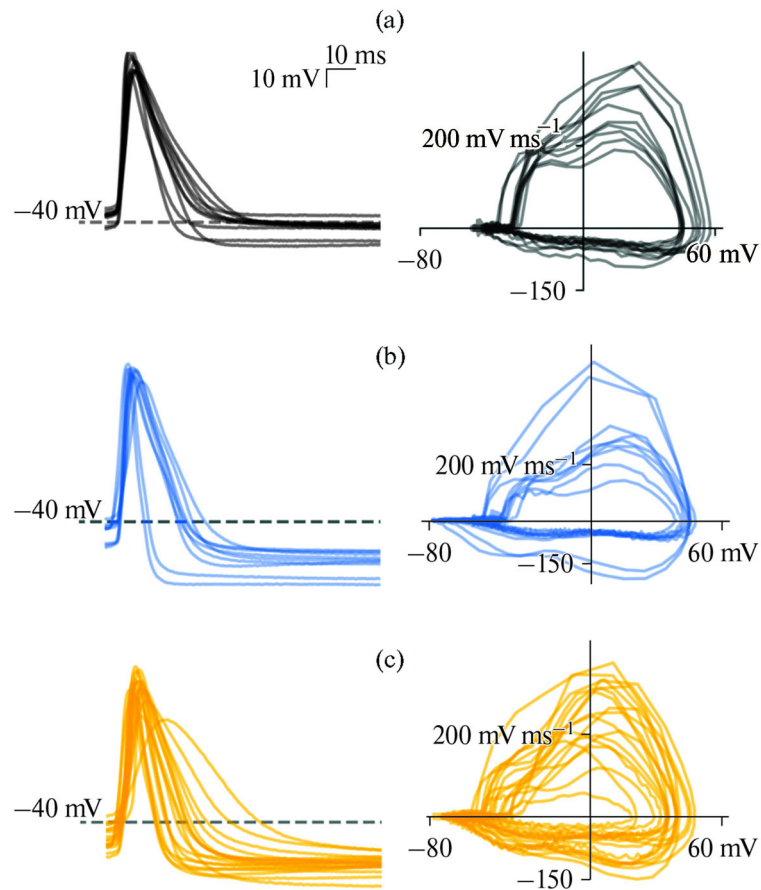


Fig. 4. Superpositions of the first action potentials recorded at the rheobase current (left) and phase diagrams of the same action potentials (right).

Maximal AP generation frequency in both human neuron subtypes was higher than in rat neurons (rat: 25 ± 2 Hz; H1: 52 ± 10 Hz; H2: 46 ± 5 Hz; Fig. 3b). Meanwhile, the amplitudes of the current eliciting the AP generation at a maximal frequency were markedly lower in human neurons (rat: 456 ± 57 pA; H1: 278 ± 17 pA; H2: 84 ± 10 pA; Fig. 3d).

The elevated AP generation frequency may be due to the reduced frequency adaptation of the neurons. Thus, we analyzed the early and late AP frequency adaptation (ratio between the second and first inter-spike intervals and the last and first inter-spike intervals, respectively). The late frequency adaptation was virtually absent in both neuronal subtypes and significantly lower than in rat pyramidal cells (rat: 2.00 ± 0.10 ; H1: 1.10 ± 0.10 ; H2: 1.20 ± 0.10 ; Fig. 3g). At the same time, early frequency adaptation was not prominent in

any of the studied neuronal types (Fig. 3f). Thus, a decreased frequency adaptation may be involved in the ability of neurons in human epileptic foci in the temporal cortex to generate the APs at high frequencies.

Other potential factors that may underlie the high excitability of human neurons are the characteristics of voltage-gated currents mediating the different phases of the AP and the passive membrane properties of these neurons. To evaluate the properties of voltage-gated currents, we analyzed the single APs generated at the rheobase current.

Action potential properties of human and rat neurons

The high excitability of the human neurons may be linked to the characteristics of the voltage-gated currents mediating the different phases of the AP or the passive membrane properties of

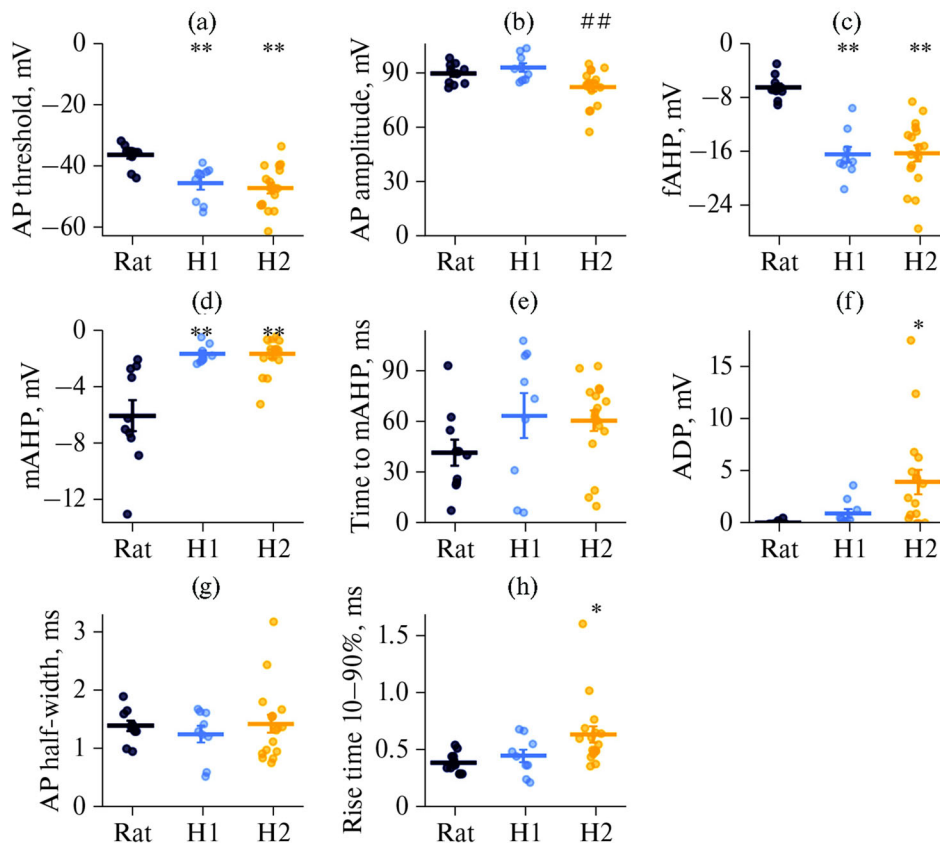


Fig. 5. Statistical analysis of the APs in human and rat neurons. (a) AP threshold. $F_{2,33} = 10.4$, $p < 0.001$; (b) AP amplitude. $F_{2,33} = 5.7$, $p < 0.01$; (c) Fast AHP amplitude. $F_{2,33} = 22.0$, $p < 0.0001$; (d) Medium AHP amplitude. $F_{2,31} = 15.3$, $p < 0.0001$; (e) Time to medium AHP peak. $F_{2,31} = 1.7$, $p = 0.2$; (f) Afterdepolarization amplitude. $F_{2,33} = 4.8$, $p < 0.05$; (g) AP half-width. $F_{2,33} = 0.37$, $p = 0.7$; (h) AP rise time from 10% to 90% of the amplitude. $F_{2,33} = 4.23$, $p < 0.05$; *— $p < 0.05$, **— $p < 0.01$ —differences between rat and human neurons; ##— $p < 0.01$ —differences between H1 and H2 neurons (Tukey's post-hoc test).

these neurons. To assess the properties of the voltage-gated currents, we analyzed the characteristics of the single APs generated at the rheobase current in the studied neurons. The examples of action potentials are shown in Fig. 4 (left panels). We also plotted the phase diagrams for these APs, which helps to compare the AP thresholds and the AHP amplitudes (Fig. 4, right panels). We observed lower AP thresholds in human neurons than in rat neurons (rat: -36.6 ± 1.2 mV; H1: -45.8 ± 2.0 mV; H2: -47.3 ± 1.7 mV; Figs. 4, 5a).

This shift in the thresholds may be explained by the activation of the voltage-gated Na^+ channels at the lower voltages. We also observed the increased fast AHP amplitudes in these neurons (rat: -6.3 ± 0.6 mV; H1: -16.3 ± 1.2 mV; H2: -16.2 ± 1.2 mV; Fig. 5c), whereas the medium AHP was virtually absent (rat: -6.0 ± 1.1 mV; H1:

-1.7 ± 0.2 mV; H2: -1.7 ± 0.3 mV; Figs. 4, 5d, 6). Fast AHP mediated by the big-conductance calcium-dependent K^+ channels (BK-channels) shortens the inter-spike intervals and leads to an increased AP frequency in response to the depolarization of a neuronal membrane [18, 19]. Thus, it can serve as one of the mechanisms leading to the increased excitability of neurons in human epileptic foci.

In H2 neurons, we also observed the afterdepolarization that was absent in rat pyramidal cells and H1 neurons (rat: 0.10 ± 0.10 mV; H1: 1.0 ± 0.4 mV; H2: 4.0 ± 1.2 mV; Fig. 5f). Another property of H2 neurons was a relatively slow AP rise phase. Rise time from 10% to 90% of the maximal amplitude in these neurons was longer than in rat pyramidal cells (rat: 0.40 ± 0.10 ms; H1: 0.5 ± 0.2 ms; H2: 0.60 ± 0.10 ms; Fig. 5h), while the

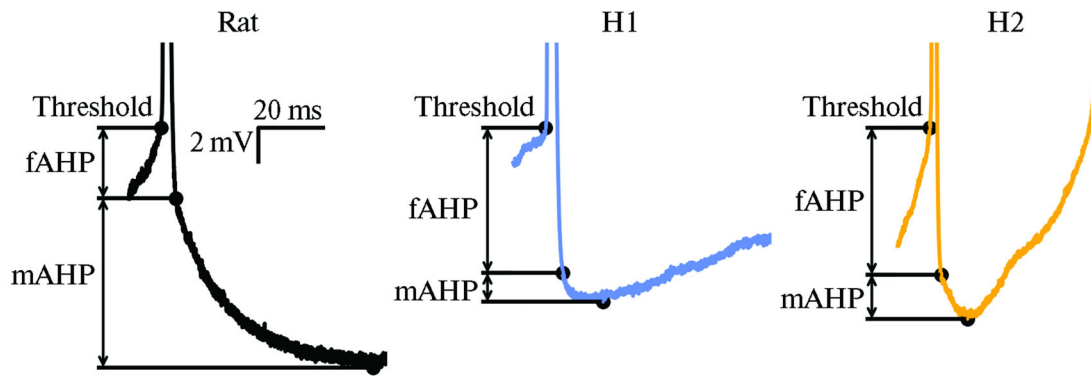


Fig. 6. AHP shape in rat and human neurons. fAHP—fast AHP; mAHP—medium AHP.

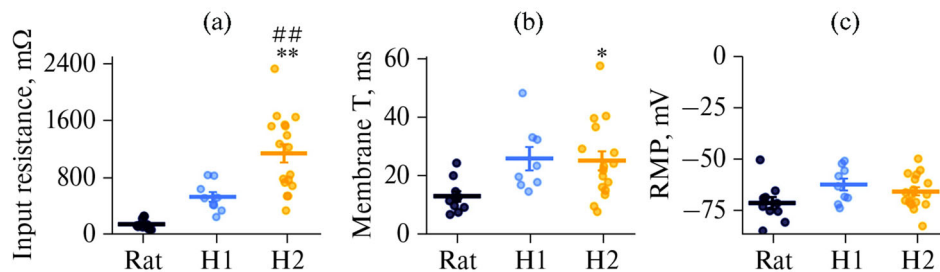


Fig. 7. Statistical analysis of the passive membrane properties in human and rat neurons. (a) Membrane input resistance. $F_{2,33} = 21.9$, $p < 0.0001$; (b) Membrane time constant. $F_{2,31} = 4.5$, $p < 0.05$; (c) Resting membrane potential. $F_{2,33} = 2.6$, $p = 0.09$; *— $p < 0.05$, **— $p < 0.01$ —differences between the human and rat neurons; ##— $p < 0.01$ —differences between the H1 and H2 neurons (Tukey's post-hoc test).

half-width was similar for all three studied types of neurons (Fig. 5g).

Passive biophysical membrane properties of neurons

Apart from the properties of voltage-gated currents mediating the AP generation, elevated excitability of neurons in the epileptic foci in the temporal cortex of refractory temporal lobe epilepsy patients may be attributed to their passive membrane properties. Thus, we analyzed such membrane properties of the neurons as their input resistance, membrane time constant, and resting membrane potential.

We discovered that most human neurons had higher input resistance than rat neurons, although the significant difference was observed only for H2 neurons (rat: 149 ± 24 MOhm; H1: 543 ± 70 MOhm; H2: 1172 ± 133 MOhm, Fig. 7a). Input resistance defines the magnitude of the depolarization response of the neuronal membrane to the inward current of a given amplitude. Thus, the higher it is, the more excitable such neuron must be.

High input resistance may be due to the decreased area of the neuronal membrane or to the reduced density of active ion channels on it. Thus, a significant membrane area reduction may happen when part of the dendrite tree is cut off when preparing the brain slices. The membrane area may be assessed by its capacitance, which affects the membrane time constant. Human neurons had a higher membrane time constant than rat cortical pyramidal cells, indicating a higher membrane area (rat: 13.2 ± 1.8 ms; H1: 26.1 ± 4.0 ms; H2: 25.4 ± 3.3 ms; Fig. 7b). These values are consistent with published data for humans [11, 20–24] and rat [9] neurons. This indicates that the truncated dendrite tree is unlikely to cause high membrane input resistance.

The main conductance contributing to the resting membrane input resistance is mediated by the leak K^+ currents, which define the resting membrane potential of the neurons. Thus, the change in the density of active K^+ channels may lead to a shift in the ionic balance and affect the resting

membrane potential of the membrane. However, in both types of human neurons, the resting membrane potential was similar to that in rat prefrontal cortex pyramidal cells (Fig. 7c). It matched the values published earlier for human neurons [11, 23–25].

DISCUSSION

In this work, we obtained the brain tissue samples from 4 patients with childhood refractory temporal lobe epilepsy and 4 rats. In acute slices prepared from these samples, we recorded the membrane properties of 26 human neurons and 10 rat pyramidal cells. Human neurons were divided into two electrophysiological types based on their response pattern to the depolarizing current. The H1 neurons were characterized by the relatively slow increase of the action potential frequency with the rise of the depolarizing current and its lower maximal values. In H2 neurons, we observed a more prominent AHP, and the AP rise time in these neurons was longer than in H1 neurons. Also, H2 neurons in the human temporal cortex had a higher input resistance. In contrast with the earlier published data, the input resistance in the studied human neurons was very high, 4 to 10 times higher than in rat pyramidal cells.

Methodical limitations

The heterogeneity of the brain samples limits the interpretation of the results of this work. The samples were obtained from patients of different ages, sex, and disease etiology. For this reason, the characteristics of the neurons in different patients may be heterogeneous. In our work, we distinguished two electrophysiological types of neurons. Still, no link between the neuronal properties and patient clinical data was observed, so we assume that this classification is not due to the difference between the patients.

The brain slice preparation technique from the post-surgery material may also be a source of some variability in the registered neuronal properties. First, the cortical area to be removed was chosen based on the location of the epileptic foci and was different for each patient. Second, during the surgery, the removed tissue is subject to

mechanical deformation, high temperature from the electrocoagulation, and unavoidable ischemia. These impacts were minimized as much as possible during the surgery but can not be avoided completely. Third, after the removal, the tissue sample is transported to the laboratory for the acute slice preparation, which takes 30–60 minutes. All of the above factors lead to neuronal death, so the survived neurons might not be fully representative.

However, this is unlikely to account for such observed parameters of the neurons as high input resistance and high AP generation frequency, as the neurons with such properties are absent in the reported samples from human and rat brains, so the likelihood of them being the result of a specific selection is low. Although most of the authors used a sucrose-based solution for slice preparation and tissue transportation [26–30] instead of the ICSF, our technique for the acute slice preparation is similar to that used by the other authors.

Features of refractory epilepsy in children

All patients were recommended to remove the epileptic foci for treatment of the refractory temporal lobe epilepsy. This approach is considered justified when the seizures remain resistant to a minimum of two different pharmacological protocols and keep severely affecting the patient's quality of life. The surgical treatment of epilepsy at a young age provides the most favorable prognosis for the child's quality of life and subsequent cognitive development [4]. Currently, a range of potential mechanisms that could lead to pharmacoresistant epileptic seizures, including the genetic, transporter, network, and some others, is described in the literature [31]. Thus, an elevated expression of the P-glycoproteins in the endothelial cells and astrocytes was demonstrated in the brain tissue of patients with refractory epilepsy [32]. P-glycoproteins mediate the transport of different pharmacological agents, including the antiepileptic drugs, in the blood, thus lowering the blood–brain barrier permeability for these substances [2]. This may lead to lowering the antiepileptic drug concentrations in the brain tissue below the effective range and the development of pharmacoresistance. Another potential mechanism is seizure-induced changes in the properties

or distribution of the pharmacological targets of antiepileptic drugs [33]. Thus, it was demonstrated that the block of the open Na^+ channels by carbamazepine was absent in neurons of the temporal cortex of patients with carbamazepine-resistant seizures, in contrast to the patients for whom this drug was effective [34]. However, such evidence does not exist for all medications that the patients included in this study received. The early age of the onset of refractory epilepsy may point to its genetic mechanism. However, all patients in this work had acquired epilepsy linked to such factors as trauma, inflammatory diseases, and brain tumors, so the shared genetic mechanism for these cases is unlikely.

Electrophysiological types of neurons identified in the human temporal cortex

All recorded neurons in the human temporal cortex were divided into two electrophysiological types. We did not perform the morphological reconstruction of these neurons, so determining their morphological type is impossible. However, we can presume that one of these groups corresponds to a population of excitatory pyramidal cells. The other is a sample of different neurons of the other types, presumably inhibitory. The properties of the action potentials are markedly different for pyramidal cells and interneurons in rats. Rat interneurons demonstrate a higher action potential frequency than pyramidal cells, faster kinetics of the APs, and more pronounced AHP [35]. Similar differences between the membrane properties of excitatory and inhibitory neurons are observed in long-tailed macaques [36]. The relatively high AP generation frequencies and high input resistance relative to the pyramidal cells in the same area were earlier demonstrated in the interneurons in the temporal cortex of patients with temporal lobe epilepsy [37]. We have observed high AHP amplitudes and lack of frequency adaptation in both studied types of neurons, which does not allow us to confidently match these two groups with any populations of neurons described in the literature. These features are probably linked to the physiological immaturity of the neurons in children's brains, which makes their properties from those observed in adult patients. Another possible explanation is

that both types of neurons belong to one morphophysiological type but differ by either subtype, physiological state, or maturity level. We need further experiments with morphological reconstruction of the studied neurons to answer this question.

Neurons in human epileptic foci had a high input resistance

We observed an extremely high input resistance in neurons in the human temporal cortex of patients with refractory epilepsy. It was 4–10 times higher than in rat pyramidal cells. Such a feature led to the increased excitability of neurons in the epileptic foci. The high excitability of neurons may feature the pathological change in brain tissue in the epileptic foci; however, earlier published data obtained from the post-surgery material from refractory epilepsy patients did not report this feature. Thus, Berg et al. conducted a cluster analysis of the transcriptomic and physiological subtypes of pyramidal cells in the human temporal cortex and discerned five different subtypes, only one of which had input resistance in the order of 300 M Ω . In contrast, for the rest of the subtypes, this parameter had values around 100–150 M Ω [26]. Banerjee et al. studied the electrophysiological properties of neurons from the areas with focal cortical dysplasia and reported the input resistance values of 174 ± 21 M Ω [20]. Very close values (153.2 ± 27.3 M Ω) were observed in neurons of II–III layers of temporal cortex in adult patients with pharmacoresistant temporal lobe epilepsy [21], as well as epilepsy or brain tumors [22]. Comparison of cortical neurons in rats and humans have shown differences in input resistance before. Still, these differences were either moderate (63.8 ± 4.5 M Ω in rats and 86.1 ± 8.1 M Ω in humans) [23], or insignificant (38.8 ± 21.4 M Ω in rats and 43.3 ± 24.5 M Ω in humans) [24]. Another possible cause of this feature may be the childhood age of the patients included in this study. Most of the published literary data was obtained from the tissue samples from adult patients. Tasker et al. report the input resistance of neurons in children's brain tissue samples around 70 M Ω , which is lower than we observed in rat neurons [11]. However, they used the sharp microelectrode registration tech-

nique. This technique is limited by the high series resistance of the electrodes on the one hand and the significant leak current at the point of contact between the electrode and the membrane on the other, which leads to the underestimation of the input resistance of neuronal membranes. We hypothesize that the input resistance values registered in neurons in the temporal cortex are specific to the cases of childhood epilepsy.

Human neurons demonstrated high action potential frequency

High input resistance in human cortical neurons led to their elevated excitability. Thus, relatively low in comparison with the rat neurons values of rheobase current and minimal current eliciting the depolarization block are probably explained by the high input resistance. On the other hand, human neurons demonstrated such features as lack of frequency adaptation and high maximal AP frequency. Frequency adaptation in neurons depends on BK channels and M-type K^+ channels [38]. Thus, lack of frequency adaptation in neurons may be linked to either lack or dysfunction of these channels. There is evidence that the hereditary dysfunction of the M-type K^+ channels is related to idiopathic epilepsy [39]. BK channel dysfunctions may lead to movement disorders [40]. It is possible that the lack of these channels in the studied neurons is due to their physiological subtype; however, we consider it improbable that the pyramidal cells, which make up around 80% of the neuronal population in the cortex, were virtually absent in our random sample. Most likely, at least a significant portion of the studied neurons are pyramidal cells that demonstrated the lack of frequency adaptation.

Neurons in the human temporal cortex containing the epileptic foci had low-threshold action potentials and fast AHP

Most of the studied neurons in the human temporal cortex demonstrated low AP generation thresholds compared to the rat neurons. The AP threshold is determined by the properties of voltage-gated Na^+ channels in the axon initial segment. A low AP threshold means that the Na^+ channels open in response to a smaller depolarization of the membrane, which must lead to the

hyperexcitability of the neuron. The expression of different voltage-gated Na^+ channel isoforms is subject to change during ontogenesis. The mutations in the $Na_v1.6$ isoform are linked to the various CNS pathologies, including refractory temporal lobe epilepsy [41]. Earlier, the increased AP generation thresholds were demonstrated in the lithium-pilocarpine model in rats on the first day after the pilocarpine-induced seizures [9]. However, these changes are attributed to the acute consequences of the seizures and the early phase of epileptogenesis. Thus, they may differ from the changes in the epileptic brain. Numura et al. in their work compared the AP parameters in rat neurons and neurons in patients with temporal lobe epilepsy, and they did not report any significant differences between the AP thresholds in these neurons; they were -33.0 ± 1.9 mV for rat neurons, -31.1 ± 2.9 mV for human neurons in the morphologically normal areas, and -44.4 ± 6.1 mV for human neurons in the regions with focal cortical dysplasia ($p = 0.064$) [42]. Thus, the observed negative shift of the action potential generation thresholds in our study may be evidence of the pathological changes in the Na^+ channel functioning, both hereditary and due to epileptogenesis.

Another characteristic feature in neurons in the human temporal cortex was high fast AHP amplitude, whereas the medium AHP in these neurons was virtually absent. The increase in the relative contribution of the fast AHP phase mediated by the BK channels may contribute to neuronal hyperexcitability by reducing the interspike intervals [18, 19]. On the other hand, high fast AHP amplitudes are characteristic of interneurons in rodents [35] and primates [36]. However, as mentioned before, it is unlikely that all of the studied neurons are interneurons. Thus, this feature is probably evident of the big contribution of BK channels in the AHP on human neurons in the epileptic foci may lead to their elevated excitability.

AUTHORS' CONTRIBUTION

Malkis S.L.—electrophysiological experiments, data analysis, writing of the article.
Khachatryan V.A.—surgery, writing of the article.

Fedorov E.V.—clinical data analysis, writing of the article. Zaitsev A.V.—experimental design, discussion of the results, writing of the article.

FUNDING

The work was supported by the RSF grant no. 20-75-00131.

CONFLICT OF INTEREST

The authors declare no explicit or potential conflicts of interest in the publishing of this paper.

REFERENCES

1. Fiest KM, Sauro KM, Wiebe S, Patten SB, Kwon C-S, Dykeman J, Pringsheim T, Lorenzetti DL, Jetté N (2017) Prevalence and incidence of epilepsy: A systematic review and meta-analysis of international studies. *Neurology* 88:296–303. <https://doi.org/10.1212/WNL.0000000000003509>
2. Löscher W, Potschka H, Sisodiya SM, Vezzani A (2020) Drug Resistance in Epilepsy: Clinical Impact, Potential Mechanisms, and New Innovative Treatment Options. *Pharmacol Rev* 72:606–638. <https://doi.org/10.1124/pr.120.019539>
3. Braun KPJ (2017) Preventing cognitive impairment in children with epilepsy. *Curr Opin Neurol* 30:140–147. <https://doi.org/10.1097/WCO.0000000000000424>
4. Jayalakshmi S, Vooturi S, Gupta S, Panigrahi M (2017) Epilepsy surgery in children. *Neurology India* 65:485. https://doi.org/10.4103/neuroindia.NI_1033_16
5. Englot DJ, Rolston JD, Wang DD, Sun PP, Chang EF, Auguste KI (2013) Seizure outcomes after temporal lobectomy in pediatric patients. *J Neurosurg Pediatr* 12:134–141. <https://doi.org/10.3171/2013.5.PEDS12526>
6. Curia G, Lucchi C, Vinet J, Gualtieri F, Marinelli C, Torsello A, Costantino L, Biagini G (2014) Pathophysiology of mesial temporal lobe epilepsy: Is prevention of damage antiepileptogenic? *Current Medicinal Chemistry* 21:663–88.
7. Albrecht J, Zielińska M (2017) Mechanisms of Excessive Extracellular Glutamate Accumulation in Temporal Lobe Epilepsy. *Neurochem Res* 42:1724–1734. <https://doi.org/10.1007/s11064-016-2105-8>
8. Wong-Kissel LC, Blauwblomme T, Ho M-L, Boddaert N, Parisi J, Wirrell E, Nabout R (2018) Challenges in managing epilepsy associated with focal cortical dysplasia in children. *Epilepsy Res* 145:1–17. <https://doi.org/10.1016/j.eplepsyres.2018.05.006>
9. Smirnova EY, Amakhin DV, Malkin SL, Chizhov AV, Zaitsev AV (2018) Acute Changes in Electrophysiological Properties of Cortical Regular-Spiking Cells Following Seizures in a Rat Lithium–Pilocarpine Model. *Neuroscience* 379:202–215. <https://doi.org/10.1016/j.neuroscience.2018.03.020>
10. Huberfeld G, Blauwblomme T, Miles R (2015) Hippocampus and epilepsy: Findings from human tissues. *Revue Neurologique* 171:236–251. <https://doi.org/10.1016/j.neurol.2015.01.563>
11. Tasker JG, Hoffman NW, Kim YI, Fisher RS, Peacock WJ, Dudek FE (1996) Electrical properties of neocortical neurons in slices from children with intractable epilepsy. *J Neurophysiol* 75:931–939. <https://doi.org/10.1152/jn.1996.75.2.931>
12. Kroon T, van Hugte E, van Linge L, Mansvelder HD, Meredith RM (2019) Early postnatal development of pyramidal neurons across layers of the mouse medial prefrontal cortex. *Sci Rep* 9:5037. <https://doi.org/10.1038/s41598-019-41661-9>
13. Juraska JM, Drzewiecki CM (2020) Cortical reorganization during adolescence: What the rat can tell us about the cellular basis. *Dev Cogn Neurosci* 45:100857. <https://doi.org/10.1016/j.dcn.2020.100857>
14. Harris CR, Millman KJ, van der Walt SJ, Gommers R, Virtanen P, Cournapeau D, Wieser E, Taylor J, Berg S, Smith NJ, Kern R, Picus M, Hoyer S, van Kerkwijk MH, Brett M, Haldane A, del Rio JF, Wiebe M, Peterson P, Gérard-Marchant P, Sheppard K, Reddy T, Weckesser W, Abbasi H, Gohlke C, Oliphant TE (2020) Array programming with NumPy. *Nature* 585:357–362. <https://doi.org/10.1038/s41586-020-2649-2>
15. Virtanen P, Gommers R, Oliphant TE, Haberland M, Reddy T, Cournapeau D, Burovski E, Peterson P, Weckesser W, Bright J, van der Walt SJ, Brett M, Wilson J, Millman KJ, Mayorov N, Nelson ARJ, Jones E, Kern R, Larson E, Carey CJ, Polat İ, Feng Y, Moore EW, VanderPlas J, Laxalde D, Perktold J, Cimrman R, Henriksen I, Quintero EA, Harris CR, Archibald AM, Ribeiro AH, Pedregosa F, van Mulbregt P, SciPy 1.0 Contributors (2020) SciPy 1.0: Fundamental algorithms for scientific computing in Python. *Nat Methods* 17:261–272. <https://doi.org/10.1038/s41592-019-0686-2>

16. Campagnola L, Kratz MB, Manis PB (2014) ACQ4: An open-source software platform for data acquisition and analysis in neurophysiology research. *Front Neuroinform* 8:3. <https://doi.org/10.3389/fninf.2014.00003>
17. Hunter JD (2007) Matplotlib: A 2D Graphics Environment. *Comput Sci Eng* 9:90–95. <https://doi.org/10.1109/MCSE.2007.55>
18. Jaffe DB, Brenner R (2018) A computational model for how the fast afterhyperpolarization paradoxically increases gain in regularly firing neurons. *J Neurophysiol* 119:1506–1520. <https://doi.org/10.1152/jn.00385.2017>
19. Gu N, Vervaeke K, Storm JF (2007) BK potassium channels facilitate high-frequency firing and cause early spike frequency adaptation in rat CA1 hippocampal pyramidal cells. *J Physiol* 580:859–882. <https://doi.org/10.1113/jphysiol.2006.126367>
20. Banerjee J, Dey S, Dixit AB, Doddamani R, Sharma MC, Garg A, Chandra PS, Tripathi M (2020) GABAA Receptor-Mediated Epileptogenicity in Focal Cortical Dysplasia (FCD) Depends on Age at Epilepsy Onset. *Front Cell Neurosci* 14:562811. <https://doi.org/10.3389/fncel.2020.562811>
21. Lehnhoff J, Strauss U, Wierschke S, Grosser S, Pollali E, Schneider UC, Holtkamp M, Dehnicke C, Deisz RA (2019) The anticonvulsant lamotrigine enhances Ih in layer 2/3 neocortical pyramidal neurons of patients with pharmacoresistant epilepsy. *Neuropharmacology* 144:58–69. <https://doi.org/10.1016/j.neuropharm.2018.10.004>
22. Bocchio M, Lukacs IP, Stacey R, Plaha P, Apostolopoulos V, Livermore L, Sen A, Ansoorge O, Gillies MJ, Somogyi P, Capogna M (2018) Group II Metabotropic Glutamate Receptors Mediate Presynaptic Inhibition of Excitatory Transmission in Pyramidal Neurons of the Human Cerebral Cortex. *Front Cell Neurosci* 12:508. <https://doi.org/10.3389/fncel.2018.00508>
23. Verhoog MB, Goriounova NA, Obermayer J, Stroeder J, Hjorth JJJ, Testa-Silva G, Baayen JC, de Kock CPJ, Meredith RM, Mansvelder HD (2013) Mechanisms Underlying the Rules for Associative Plasticity at Adult Human Neocortical Synapses. *J Neurosci* 33:17197–17208. <https://doi.org/10.1523/JNEUROSCI.3158-13.2013>
24. Teichgräber LA, Lehmann T-N, Meencke H-J, Weiss T, Nitsch R, Deisz RA (2009) Impaired function of GABAB receptors in tissues from pharmacoresistant epilepsy patients. *Epilepsia* 50:1697–1716. <https://doi.org/10.1111/j.1528-1167.2009.02094.x>
25. Tóth K, Hofer KT, Kandrás Á, Entz L, Bagó A, Eröss L, Jordán Z, Nagy G, Sólyom A, Fabó D, Ulbert I, Wittner L (2018) Hyperexcitability of the network contributes to synchronization processes in the human epileptic neocortex. *J Physiol (Lond)* 596:317–342. <https://doi.org/10.1113/JP275413>
26. Berg J, Sorensen SA, Ting JT, Miller JA, Chartrand T, Buchin A, Bakken TE, Budzillo A, Dee N, Ding S-L, Gouwens NW, Hodge RD, Kalmbach B, Lee C, Lee BR, Alfiler L, Baker K, Barkan E, Beller A, Berry K, Bertagnolli D, Bickley K, Bomben J, Braun T, Brouner K, Casper T, Chong P, Crichton K, Dalley R, de Frates R, Desta T, Lee SD, D’Orazi F, Dotson N, Egdorf T, Enstrom R, Farrell C, Feng D, Fong O, Furdan S, Galakhova AA, Gamlin C, Gary A, Glandon A, Goldy J, Gorham M, Goriounova NA, Gratiy S, Graybuck L, Gu H, Hadley K, Hansen N, Heistek TS, Henry AM, Heyer DB, Hill D, Hill C, Hupp M, Jarsky T, Kebede S, Keene L, Kim L, Kim M-H, Kroll M, Latimer C, Levi BP, Link KE, Mallory M, Mann R, Marshall D, Maxwell M, McGraw M, McMillen D, Melief E, Mertens EJ, Mezei L, Mihut N, Mok S, Molnar G, Mukora A, Ng L, Ngo K, Nicovich PR, Nyhus J, Olah G, Oldre A, Omstead V, Ozsvar A, Park D, Peng H, Pham T, Pom CA, Potekhina L, Rajanbabu R, Ransford S, Reid D, Rimorin C, Ruiz A, Sandman D, Sulc J, Sunkin SM, Szafer A, Szemenyei V, Thomsen ER, Tieu M, Torkelson A, Trinh J, Tung H, Wakeman W, Waleboer F, Ward K, Wilbers R, Williams G, Yao Z, Yoon J-G, Anastasiou C, Arkhipov A, Barzo P, Bernard A, Cobbs C, de Witt Hamer PC, Ellenbogen RG, Esposito L, Ferreira M, Gwinn RP, Hawrylycz MJ, Hof PR, Idema S, Jones AR, Keene CD, Ko AL, Murphy GJ, Ng L, Ojemann JG, Patel AP, Phillips JW, Silbergeld DL, Smith K, Tasic B, Yuste R, Segev I, de Kock CPJ, Mansvelder HD, Tamas G, Zeng H, Koch C, Lein ES (2021) Human neocortical expansion involves glutamatergic neuron diversification. *Nature* 598:151–158. <https://doi.org/10.1038/s41586-021-03813-8>
27. Levinson S, Tran CH, Barry J, Viker B, Levine MS, Vinters HV, Mathern GW, Cepeda C (2020) Paroxysmal Discharges in Tissue Slices From Pediatric Epilepsy Surgery Patients: Critical Role of GABAB Receptors in the Generation of Ictal Activity. *Front Cell Neurosci* 14:54. <https://doi.org/10.3389/fncel.2020.00054>
28. Kraus L, Monni L, Schneider UC, Onken J,

- Spindler P, Holtkamp M, Fidzinski P (2020) Preparation of Acute Human Hippocampal Slices for Electrophysiological Recordings. *J Vis Exp* 159: e61085. <https://doi.org/10.3791/61085>
29. Kandrás Á, Hofer KT, Tóth K, Tóth EZ, Entz L, Bagó AG, Eröss L, Jordán Z, Nagy G, Fabó D, Ulbert I, Wittner L (2019) Presence of synchrony-generating hubs in the human epileptic neocortex. *J Physiol JP278499*. <https://doi.org/10.1113/JP278499>
 30. Holtkamp D, Opitz T, Niespodziany I, Wolff C, Beck H (2017) Activity of the anticonvulsant lacosamide in experimental and human epilepsy via selective effects on slow Na⁺ channel inactivation. *Epilepsia* 58:27–41. <https://doi.org/10.1111/epi.13602>
 31. Tang F, Hartz AMS, Bauer B (2017) Drug-Resistant Epilepsy: Multiple Hypotheses, Few Answers. *Front Neurol* 8:301. <https://doi.org/10.3389/fneur.2017.00301>
 32. Kwan P, Brodie MJ (2005) Potential role of drug transporters in the pathogenesis of medically intractable epilepsy. *Epilepsia* 46:224–235. <https://doi.org/10.1111/j.0013-9580.2005.31904.x>
 33. Remy S, Beck H (2006) Molecular and cellular mechanisms of pharmacoresistance in epilepsy. *Brain* 129:18–35. <https://doi.org/10.1093/brain/awh682>
 34. Remy S, Gabriel S, Urban BW, Dietrich D, Lehmann TN, Elger CE, Heinemann U, Beck H (2003) A novel mechanism underlying drug resistance in chronic epilepsy. *Ann Neurol* 53:469–479. <https://doi.org/10.1002/ana.10473>
 35. Malkin SL, Kim KK, Tikhonov DB, Zaitsev AV (2014) Properties of spontaneous and miniature excitatory postsynaptic currents in neurons of the rat prefrontal cortex. *Journal of Evolutionary Biochemistry and Physiology* 50(6): 506–514. <https://doi.org/10.1134/S0022093014060052>
 36. Krimer LS, Zaitsev AV, Czanner G, Kröner S, González-Burgos G, Povysheva NV, Iyengar S, Barrionuevo G, Lewis DA (2005) Cluster Analysis–Based Physiological Classification and Morphological Properties of Inhibitory Neurons in Layers 2–3 of Monkey Dorsolateral Prefrontal Cortex. *Journal of Neurophysiology* 94:3009–3022. <https://doi.org/10.1152/jn.00156.2005>
 37. Menendez de la Prida L, Benavides-Piccione R, Sola R, Pozo MA (2002) Electrophysiological properties of interneurons from intraoperative spiking areas of epileptic human temporal neocortex. *Neuroreport* 13:1421–1425. <https://doi.org/10.1097/00001756-200208070-00015>
 38. Benda J, Herz AVM (2003) A universal model for spike-frequency adaptation. *Neural Comput* 15:2523–2564. <https://doi.org/10.1162/089976603322385063>
 39. Neubauer BA, Waldegger S, Heinzinger J, Hahn A, Kurlemann G, Fiedler B, Eberhard F, Muhle H, Stephani U, Garkisch S, Eeg-Olofsson O, Müller U, Sander T (2008) KCNQ2 and KCNQ3 mutations contribute to different idiopathic epilepsy syndromes. *Neurology* 71:177–183. <https://doi.org/10.1212/01.wnl.0000317090.92185.ec>
 40. Miller JP, Moldenhauer HJ, Keros S, Meredith AL (2021) An emerging spectrum of variants and clinical features in KCNMA1-linked channelopathy. *Channels (Austin)* 15:447–464. <https://doi.org/10.1080/19336950.2021.1938852>
 41. Zybura A, Hudmon A, Cummins TR (2021) Distinctive Properties and Powerful Neuromodulation of Nav1.6 Sodium Channels Regulates Neuronal Excitability. *Cells* 10:1595. <https://doi.org/10.3390/cells10071595>
 42. Nomura S, Kida H, Hirayama Y, Imoto H, Inoue T, Moriyama H, Mitsushima D, Suzuki M (2019) Reduction of spike generation frequency by cooling in brain slices from rats and from patients with epilepsy. *J Cereb Blood Flow Metab* 39:2286–2294. <https://doi.org/10.1177/0271678X18795365>